Nanotubes

DOI: 10.1002/ange.200502591

Characteristics of Boron Nitride Nanotube–Polyaniline Composites**

Chunyi Zhi, Yoshio Bando, Chengchun Tang, Susumu Honda, Kazuhiko Sato, Hiroaki Kuwahara, and Dmitri Golberg*

Significant efforts have been made to design and fabricate nanotube-based composites since the pioneering report on carbon nanotube (CNT)–polymer composites by Ajayan et al.[1] These composites are expected to have useful electrical and optical properties, thermal conductivity, and superior mechanical strength compared to unprocessed polymers.[2,3] Polyaniline (PANI), a typical electroconductive polymer, is a promising candidate for the fabrication of nanotube-based composites due to its stability and redox properties. Significant progress has been achieved with respect to the processing and property improvements of PANI–CNT composites.[4] For real-device applications, the two important factors—functionality and processability—should be considered. These parameters primarily depend on the efficiency of interactions between the nanotubes and polymer chains within a composite material. To enhance these interactions, the PANI–CNT composites are typically fabricated by in situ polymerization.

Boron nitride nanotubes (BNNTs), which are structurally similar to CNTs, have been predicted to behave like wide-band-gap semiconductors independent of radius, chirality, and the number of tubular shells.[5] Interestingly, the electrical polarization induced by broken symmetry along the BNNT axis has been predicted in a theoretical study; this is quite distinct from the case of CNTs.[6] Moreover, BNNTs have superb mechanical properties, thermal conductivity, and resistance to oxidation at high temperatures.[7–11] These factors may promote effective BNNT usage in nanocomposites. However, to the best of our knowledge, no BNNT–polymer composites have been reported to date. Studies of BNNTs–polymer composites are absent because it is extremely difficult to obtain a highly pure BNNT phase with a yield high enough to fabricate and test a composite

[*] Dr. C. Zhi, Prof. Y. Bando, Dr. C. Tang, Prof. D. Golberg
Advanced Materials Laboratory
National Institute for Materials Science (NIMS)
Namiki 1-1, Tsukuba, Ibaraki 305-0044 (Japan)
Fax: (+81) 29-851-6280
E-mail: zhi.chunyi@nims.go.jp
Dr. S. Honda, Dr. K. Sato, Dr. H. Kuwahara
Innovation Research Institute, Teijin Ltd.
2-1, Hinode-cho, Iwakuni, Yamaguchi 740-8511 (Japan)

[**] We thank Drs. Y. Uemura, M. Mitome, K. Kurashima, R. Z. Ma, and T. Sasaki for their cooperation and kind help.

Supporting information for this article is available on the WWW under http://www.angewandte.org or from the author.

material, although many methods have been probed to synthesize BNNTs.[12–16]

In the study presented herein, large quantities of highly pure BNNTs were synthesized by chemical vapor deposition with boron and metal oxide as the reactants.[17,18] PANI–BNNTs composites were fabricated by simple solution mixing to give self-organized composite films. Detailed comparative characterization of the composite samples and initial materials constituting them was then carried out. The morphology of the composites was analyzed by using scanning and transmission electron microscopy (SEM, TEM), which both revealed uniform coverage of a BNNT surface with PANI. Additional characterization was performed by using Raman spectroscopy, UV/Vis absorption, and X-ray diffraction (XRD). All results indicated strong interactions between PANI and BNNTs within the composites.

BNNTs and a nonconducting soluble emeraldine-based form of PANI (EB) were mixed and sonicated in *N*,*N*-dimethylformamide to form a solution. The solution was then left at room temperature for over 12 h during which a self-organized composite film formed at the bottom of the reaction vessel. It is worth noting that when the same process was carried out with a solution of CNT and EB, no film was deposited. This result indicates that BNNTs display stronger interactions with EB than CNTs. A BNNT–EB film was removed from the reaction vessel and mounted on a silicon wafer for further characterization and testing.

Figure 1 depicts typical SEM images of a composite film. Figure 1a shows the BNNTs embedded in an EB matrix; some BNNTs are out of the matrix because the film broke during its mounting on a silicon wafer. During the long irradiation times, the film shrank and broke, thus allowing the BNNTs to become clearly visible (Figure 1b). The morphology of BNNTs within the composites is similar to that of pure BNNTs, as revealed by SEM. However, notable differences were observed by TEM. Figure 2a shows a low magnification TEM image of a composite. Although the BNNTs are covered by EB, they still retain a perfect crystalline structure, as revealed by a high-resolution TEM image (Figure 2b). Typically, BNNTs are not wetted by most materials (see Supporting Information). In contrast, in the present experiments all BNNTs were well covered by EB, although some BNNTs protruded from the matrix during SEM observations. This coverage indicates strong interactions between BNNTs and EB. The origin of these interactions may be analogous to that found in a solution of BNNT/poly(*m*-phenylenevinylene-co-2,5-dioctoxy-*p*-phenylenevinylene):[19] the PANI ring units may come sufficiently close to a hexagonal BNNT surface to lead to efficient π–π interactions.[4] The interactions between BNNT and PANI are stronger than between CNT and PANI due to electrical polarization in BNNTs induced by broken symmetry.[6]

Raman spectroscopy was used to gain insight into the origin of the strong interactions between EB and BNNTs. As shown in Figure 3, two dominant peaks at 1350 and 1579 cm^{-1} are present in the Raman spectrum of pure EB. Only one peak at 1365 cm^{-1} is visible in the spectrum of BNNTs. It is surprising that the marked peak shifts are observed in the Raman spectrum of the composite. The BNNT-related peak

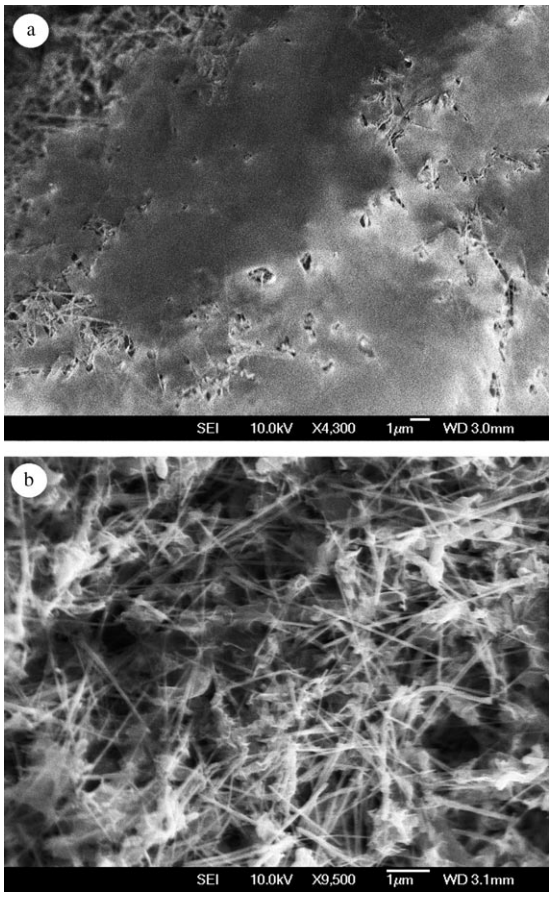

Figure 1. SEM images of an EB–BNNT composite a) before and b) after a long period (10–15 s) of electron-beam irradiation inside the scanning electron microscope.

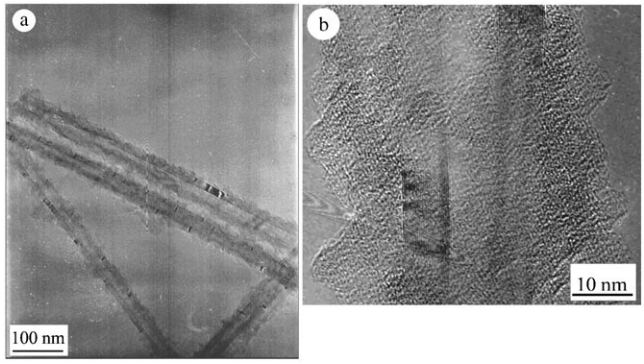

Figure 2. a) Low magnification TEM image and b) high-resolution TEM image of an EB–BNNT composite.

shifts to 1352 cm^{-1}, while the EB-related peak at 1579 cm^{-1} shifts to 1589 cm^{-1} (the peak at 1350 cm^{-1} cannot be identified in the spectrum because it is too weak and overlaps with the BNNT-related peak). Raman peak shifts have not been observed during studies of CNT–PANI composites. It is well known that the Raman spectra of CNTs consist of a G band (in-plane stretching, E_{2g} mode) and a D band induced by the disordering or an amorphous C residue. For single-walled

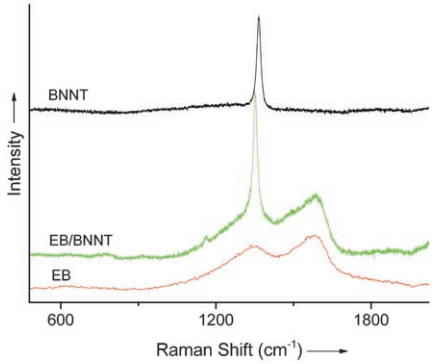

Figure 3. Raman spectra of BNNTs, EB, and an EB–BNNT composite film.

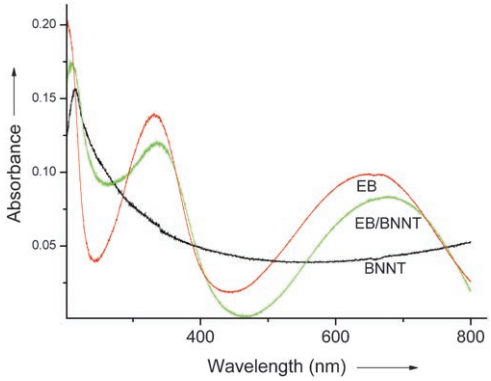

Figure 4. UV/Vis absorption spectra of BNNTs, EB, and an EB–BNNT composite film.

CNTs, evidence of a radial breathing mode (RBM) can also be observed, which is associated with a symmetric movement of all C atoms in the radial direction. The D and G bands are usually not changed in the Raman spectra of CNT–polymer composites, whereas the RBM may shift to somewhat lower frequencies. This fact is supposed to highlight that the breathing mode of single-walled CNTs is largely affected by the particular surrounding of an individual tube.[20] It is clear that a different mechanism should be assigned to explain the large Raman shifts observed in our experiments. Raman spectra are associated with the lattice vibrations. These vibrations are affected by the atomic structure, chemical bonds, and/or electronic structure through electron–phonon coupling. For BNNTs, the shifts may be caused by the prominent variations of the electronic structure rather than the atomic structure. The BNNTs are structurally stable, and it is doubtful that EB, which only covers the BNNT surface, may affect the entire atomic structure of the nanotube. For EB, the shift may be caused by conformation-induced changes in the electronic structure. Generally, given the fact that this phenomenon has not been observed for the CNT composites, we suggest that the peak shift may be related to the electrical polarization solely peculiar to BNNTs.[6] Nevertheless, strong interactions between EB and BNNTs have been demonstrated here by these Raman studies. These interactions may facilitate the charge-transfer processes between the two components. A detailed mechanism of the prominent Raman shifts for the novel composites is still not clear and is the subject of on-going research.

To reveal the influence of the interactions within the composites on the electronic structures of the constituting EB and BNNTs, we performed UV/Vis absorption measurements. Figure 4 shows the UV/Vis absorption spectra of EB, a composite film, and a BNNT film retracted from the composite film by heating the sample at 700 °C in air. For EB, two broad peaks are visible with maximums at 332 nm and 650 nm, which correspond to the π–π^* transitions centered at the benzenoid unit of EB and on the quinoid exciton band, respectively.[21] The peak at 332 nm shifts to 338 nm and that at 650 nm shifts to 673 nm for the composite. For BNNTs, the peak corresponding to a band-gap transition shifts from 214 nm (pure BNNT film) to 210 nm (composite film). This shift implies that BNNTs may have a dopant effect, which was first mentioned for CNT–PANI composites.[4b] However, it is hard to expect a drastic improvement in the conductivity of the present EB–BNNT composites as EB is a nonconducting form of PANI and BNNT is a wide-band-gap semiconductor. In CNT–PANI composites, CNTs can act as conducting bridges, which leads to an increase in conductivity, whereas the present BNNTs cannot. Further investigations on the dopant effect within the composites by using luminescence experiments are underway.

The strong interactions in the EB–BNNT composites may influence the conformation of EB.[4a] Consequently, the ordered structures of a EB–BNNT composite were investigated by XRD, as shown in Figure 5. For BNNTs, the peaks

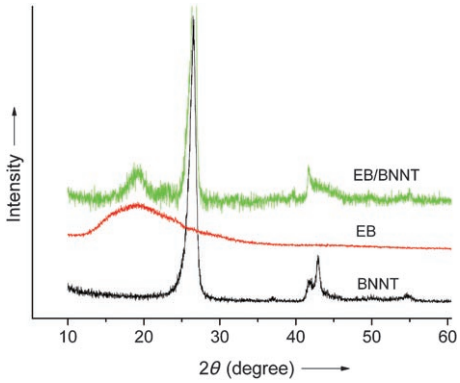

Figure 5. XRD of BNNTs, EB, and an EB–BNNT composite powder.

at $2\theta = 26°$, 41°, 43°, and 54° correspond to the (002), (100), (101), and (004) reflections, respectively. Pure EB displays only a very broad peak centered at 19°. However, for the composite, the EB-related peak becomes much sharper (the full-width half maximum decreases from 10 to 3°). This peak sharpening indicates that the structure of EB within a composite becomes more ordered. The strong nanotube–polymer interactions may lead to such ordering. The above-mentioned EB Raman shifts may be another reflection of this ordering.

In summary, BNNTs–EB composites were fabricated by using simple solution mixing. A composite film can be obtained through self-organization, which is indicative of the strong interactions between BNNT and PANI. Proof of this interaction is given by Raman, UV/Vis absorption, and XRD experiments. BNNT may exhibit a dopant effect to PANI due to charge transfer. PANI becomes more ordered in a composite with respect to its pure form. The present studies reveal that mechanically tough BNNTs may find application as an effective composite additive in EB in order to improve the polymer processing and handling due to the strong BNNT–polymer interactions. In addition, the optical properties of the newly fabricated EB–BNNT composites may be of significant interest.

Experimental Section

An induction furnace was used to synthesize BNNTs. In a typical experimental run, a mixture of MgO, FeO, and boron powder was heated in a boron nitride crucible to 1400 °C. Ammonia gas was then introduced into the system to react with gaseous Mg and Fe and gaseous B_2O_2 was produced. After two hours, a white product was collected from a BN tube attached to the reaction chamber. The BNNT–PANI composites were fabricated by simple mixing and sonication of BNNTs and EB in the *N*,*N*-dimethylformamide. A self-organized composite film was recovered from the bottom of the reaction vessel. An SEM (JEOL SM67F) was used to characterize the products. The microstructure was investigated by using a JEOL-3000F high-resolution field-emission TEM operated at 300 kV. A Reinshaw 2000 Micro-Raman system with a 30 mW Ar^+ laser of wavelength of 514 nm was used to study the lattice vibrations of the fabricated composites. The UV/Vis absorption experiments were performed by using a HITACHI U-4100 spectrometer. XRD patterns of the samples were recorded on a RINT2200 X-ray diffractometer with standard $Cu_{K\alpha}$ radiation.

Received: July 25, 2005
Published online: November 15, 2005

Keywords: boron · conducting materials · mechanical properties · nanotubes · noncovalent interactions · polymers

[1] P. M. Ajayan, O. Stephan, C. Colliex, D. Trauth, *Science* **1994**, *265*, 1212.
[2] R. Andrews, M. C. Weisenberger, *Curr. Opin. Solid State Mater. Sci.* **2004**, *9*, 31.
[3] P. J. F. Harris, *Int. Mater. Rev.* **2004**, *49*, 31.
[4] a) R. Sainz, A. M. Benito, M. T. Martinez, J. F. Galindo, J. Sotres, A. M. Baró, B. Coraze, O. Chauvet, W. K. Maser, *Adv. Mater.* **2005**, *17*, 278; b) H. Zengin, W. Zhou, J. Jin, R. Czerw, D. W. Smith, J. L. Echegoyen, D. L. Carroll, S. H. Foulger, J. Ballato, *Adv. Mater.* **2002**, *14*, 1480; c) H. J. Choi, S. J. Park, S. T. Kim, M. S. Jhon, *Diamond Relat. Mater.* **2005**, *14*, 766; d) X. Zhang, J. Zhang, Z. Liu, *Appl. Phys. A* **2005**, *80*, 1813.
[5] X. Blase, A. Rubio, S. G. Louie, M. L. Cohen, *Europhys. Lett.* **1994**, *28*, 335.
[6] E. J. Mele, P. Král, *Phys. Rev. Lett.* **2002**, *88*, 056803.
[7] E. Hernandez, C. Goze, P. Bernier, A. Rubio, *Phys. Rev. Lett.* **1998**, *80*, 4502.
[8] A. P. Suryavanshi, M. Yu, J. Wen, C. Tang, Y. Bando, *Appl. Phys. Lett.* **2004**, *84*, 2527.
[9] D. Golberg, Y. Bando, K. Kurashima, T. Sato, *Scr. Mater.* **2001**, *44*, 1561.
[10] Y. Xiao, X. H. Yan, J. X. Cao, J. W. Ding, Y. L. Mao, J. Xiang, *Phys. Rev. B* **2004**, *69*, 205415.
[11] C. W. Chang, W. Q. Han, A. Zettl, *Appl. Phys. Lett.* **2005**, *86*, 173102.
[12] N. G. Chopra, R. J. Luyken, K. Cherrey, V. H. Crespi, M. L. Cohen, S. G. Louie, A. Zettl, *Science* **1995**, *269*, 966.
[13] A. Loiseau, F. Willaime, N. Demoncy, N. Schramchenko, G. Hug, C. Colliex, H. Pascard, *Carbon* **1997**, *35*, 743.
[14] T. Laude, Y. Matsui, A. Marraud, B. Jouffrey, *Appl. Phys. Lett.* **2000**, *76*, 3239.
[15] W. Q. Han, W. Mickelson, J. Cumings, A. Zettl, *Appl. Phys. Lett.* **2002**, *81*, 1110.
[16] Y. Chen, L. T. Chadderton, J. F. Gerald, J. S. Williams, *Appl. Phys. Lett.* **1999**, *74*, 2960.
[17] C. Tang, Y. Bando, T. Sato, K. Kurashima, *Chem. Commun.* **2002**, 1290.
[18] C. Y. Zhi, Y. Bando, C. Tang, D. Golberg, *Solid State Commun.* **2005**, *135*, 67.
[19] C. Y. Zhi, Y. Bando, C. Tang, D. Golberg, R. Xie, T. Sekiguchi, *J. Am. Chem. Soc.*, accepted.
[20] Q. Zhao, H. D. Wagner, *Philos. Trans. R. Soc. London Ser. A* **2004**, *362*, 2407.
[21] S. Quillard, G. Louarn, S. Lefrant, A. G. MacDiarmid, *Phys. Rev. B* **1994**, *50*, 12496.

